Available online at www.sciencedirect.com

ScienceDirect

Physics Procedia 19 (2011) 227–232

Physics Procedia

2011 International Conference on Optics in Precision Engineering and Nanotechnology

Phase error correction for digital fringe projection profilometry

Suodong Ma[a,b], Chenggen Quan[b], Cho Jui Tay[b], Rihong Zhu[a,*], Bo Li[a]

[a]*School of Electronic and Optical Engineering, Nanjing University of Science and Technology,Xiao Lingwei Road 200, China, 210094*
[b]*Department of Mechanical Engineering, National University of Singapore,9Engineering Drive 1, Singapore, 117576*

Abstract

Non-contact structured light system which utilizes a liquid crystal display (LCD) or digital light processing (DLP) projector is widely used in 3-D surface profile measurement. In such fringe projection profilometry, the digital fringe projection and phase-shifting technique is employed. Although the accurate phase-shifting patterns is generated by a computer and projected by the LCD or DLP projector, the phase measurement error still exists and the error will affect the surface profile measurement results. In this paper, the causes of the phase error are analyzed and the subsequent error corrections are introduced when the color-encoded digital fringe projection (CFP) technique is used to retrieve the phase value. Experimental works are also carried out to verify the effectiveness of the proposed method.

Keywords: Digital fringe projection profilometry; Phase-shifting; Phase error correction

1. Introduction

With the development of modern industry and manufacturing, it is usually required to measure the surface profile of the components in the production process. Due to its advantages of fast speed, high precision, non-destruction and full-field testing, optical fringe projection technique becomes one of the most promising three-dimensional surface profile measurement methods. It can be divided into Fourier transform profilometry (FTP) [1], Phase-shifting profilometry (PSP) [2], Color-encoded fringe projection profilometry (CFPP) [3]-[4], etc. Since the high accuracy of the measurement, PSP is the first choice in the static testing environment. In contrast, FTP and CFPP are more suitable for the dynamic testing, because only one fringe pattern is required for them. Before the emergence of the liquid crystal display (LCD) or digital light processing (DLP) projector, the fringe pattern projected is mainly generated by the interferometer [5] or the raster imaging [6]. Although such kind of fringe pattern has a good sinusoidal distribution of its intensity, the experimental equipment is too complicated. When the LCD or DLP projector is introduced, it is more convenient to generate and control the fringe pattern. However, due to some

* Corresponding author. Tel.: +86-025-84315247; fax: +86-025-84315497.
E-mail address: *zhurihong@vip.sina.com* (R. Zhu).

doi:10.1016/j.phpro.2011.06.153

inherent characteristic of the electronic devices (such as gamma distortion, etc.), the captured fringe pattern is often blurred with the non-sinusoidal distribution which will result in the profile measurement error. In order to achieve a more accurate measurement result, a lot of works have been carried out [7]-[11]. S. Zhang [8] proposed a lookup table (LUT) strategy to correct the phase error caused by gamma distortion, but it needs a complicated pre-calibration process. Y. Liu et al. [10] proposed an iterative algorithm based on inverse function shift estimation (IFSE) to compensate the distorted phase as well. This method is immune to the gamma distortion and requires only one fringe pattern, but its accuracy depends on the order of the used polynomial to some extent and it considers the whole pattern is blurred with the same gamma coefficient. Y. Hu [11] established a color cross-talk model and put forward a blind color isolation method based on the iteration, however, it has a high computational complexity. Taking into account the advantages and disadvantages of the aforementioned methods, we propose a strategy to effectively correct the phase error when the phase-shifting technique is used in CFPP.

This paper is organized as follows. In section 2, we interpret the basic principles of the digital fringe projection profilometry based on CFP technique. The causes of the phase error in CFPP are analyzed in detail and the corresponding correction algorithms are introduced as well. In section 3, experimental results are given to verify the effectiveness of the proposed strategy. Section 4 concludes this paper.

2. Theoretical analysis

2.1 Digital fringe projection profilometry

A crossed-optical-axes triangulation [1] is usually used in the digital fringe projection profilometry as shown in Figure 1. The lines $E_p'E_p$ and $E_c'E_c$ are the optical axis of the LCD or DLP projector and the CCD camera respectively. They intersect at the point O on the reference plane. The normal of this reference plane is parallel with the line $E_c'E_c$. A cosine fringe pattern generated by the projector is projected onto the measured object. For the sake of simplicity, the pattern we used only varies with the x coordinate. The distorted fringe distribution, denoted as $I(x,y)$ captured by the CCD camera is:

$$I(x,y) = A(x,y) + B(x,y)\cos[2\pi fx + \varphi(x,y)] \tag{1}$$

where f is the spatial frequency of the fringe on the reference plane, $A(x,y)$ is a slowly varying component and can be called background or direct current (DC) value, $B(x,y)$ is the modulation of the fringe pattern and $\varphi(x,y)$ is the phase distribution which is corresponding with the surface profile of the measured object.

As the analysis in the reference [1], the relationship between the phase and surface profile is:

$$h(x,y) = L\cdot\varphi(x,y)/\left[2\pi Df + \varphi(x,y)\right] \tag{2}$$

where L is the distance from the entrance pupil of CCD camera to the reference plane, D is the distance between the entrance pupil of CCD and the exit pupil of projector. Once the parameters mentioned in Eq. (2) are obtained, the surface profile $h(x,y)$ can be achieved.

2.2 Color-encoded digital fringe projection technique

Because CFP technique codes three phase-shifting sinusoidal fringe patterns into the R, G, B channels of the LCD or DLP projector and forms a single color-encoded fringe pattern, it has the advantages of high accuracy and dynamic measurement in principle. The basic formulas used in CFP technique are as follows:

$$I_R(x,y) = A(x,y) + B(x,y)\cos[2\pi fx + \varphi(x,y) - 2\pi/3] \tag{3}$$

$$I_G(x,y) = A(x,y) + B(x,y)\cos[2\pi fx + \varphi(x,y)] \tag{4}$$

$$I_B(x,y) = A(x,y) + B(x,y)\cos[2\pi fx + \varphi(x,y) + 2\pi/3] \tag{5}$$

Using the traditional three-step phase-shifting algorithm, the phase value $\varphi(x,y)$ is determined [3]:

$$\varphi(x,y) = \tan^{-1}\left(\sqrt{3}\frac{I_R(x,y) - I_B(x,y)}{2I_G(x,y) - I_R(x,y) - I_B(x,y)}\right) \tag{6}$$

Moreover, the DC value $A(x,y)$ and modulation value $B(x,y)$ also can be calculated by:

$$A(x,y)=\left(I_R(x,y)+I_G(x,y)+I_B(x,y)\right)/3 \tag{7}$$

$$B(x,y)=\left[3\left(I_R(x,y)-I_B(x,y)\right)^2+\left(2I_G(x,y)-I_R(x,y)-I_B(x,y)\right)^2\right]^{1/2}/3 \tag{8}$$

It should be noted that the $\varphi(x,y)$ is usually called wrapped phase whose principal value is between -π and π in Eq. (5). The continuous phase map can be achieved after a phase unwrapping algorithm [12] is carried out. Once the real phase is obtained, the surface profile of the test object can be acquired based on Eq. (2) or through a calibration [13].

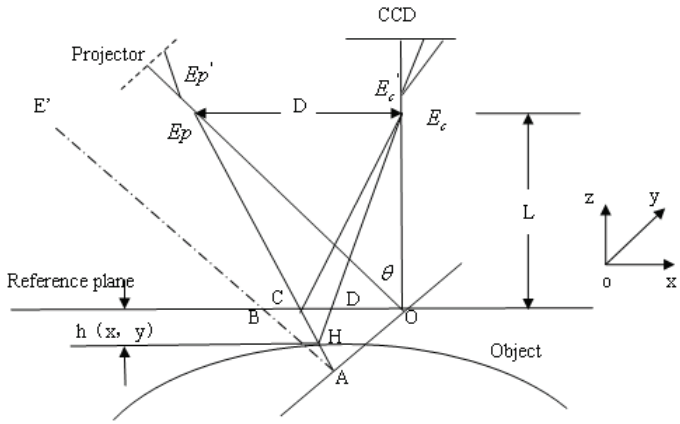

Fig. 1. Crossed-optical-axes triangulation geometry.

2.3 Phase error analysis and correction

Considering the color cross-talk effect and gamma distortion in CFPP, the fringe intensity distribution in each channel of a captured distorted pattern can be expressed as [11]:

$$I_m(x,y)=\sum_{k=0}^{K}b_{m,k}\cos\left[k\cdot(2\pi fx+\varphi(x,y)+\delta_m)\right] \tag{9}$$

where $m=R,G,B$, $b_{m,k}$ is the coefficient and δ_m represents the real phase-shifting value of different channels. When the traditional three-step phase-shifting algorithm [Eq. (6)] is utilized in CFP technique, errors will arise in the wrapped phase $\varphi(x,y)$ which can lead to the final measurement errors. That is because there are several other harmonic components in the real fringe pattern, the DC & modulation value is different between each channel, and the real phase-shifting value is not the nominal one.

In order to obtain the accurate measurements, an algorithm based on the isotropic n-dimensional fringe pattern normalization (INFPN) [14] is introduced to correct the errors from the harmonic components and the difference of DC & modulation value. After the INFPN, the fringe pattern can be rewritten as:

$$I'_m(x,y)=A'+B'\cos\left[2\pi fx+\varphi(x,y)+\delta_m\right] \tag{10}$$

A random phase-shifting algorithm (RPSA) [15]-[16] based on the iterative calculation is introduced and replaces the traditional three-step phase-shifting algorithm as well. The steps of RPSA can be summarized as follows:

Step 1. Intra-frame iteration to calculate the phase value $\varphi(x,y)$;

Step 2. Inter-frame iteration to determine the real phase-shifting value δ_m with the $\varphi(x,y)$ obtained in step 1;

Step 3. Repeats steps 1 and 2 until the algorithm converges.

3. Experimental results and discussion

To verify the effectiveness of our proposed strategy, a CFPP which is constituted by a DLP projector (Optoma EX536), a three-chip color CCD camera (CV-M9CL) and a personal computer is constructed. The projector projects

a color-encoded phase-shifting fringe pattern with a phase shift value of 120° between each color channel onto the surface of a measured object (roof-shaped object). Then the distorted fringe pattern reflected by the object is captured by the CCD camera. Figure 2(a) is the color-encoded distorted fringe pattern. The corresponding gray distorted fringe patterns of R-G-B channel are shown in Figs. 2(b)-(d), respectively. It can be seen that there is a significant difference on the stripe brightness from Fig. 2(b) to 2(d). Moreover, several other harmonic components also can be found in these patterns which form the non-sinusoidal fringe as expressed in Eq. (9).

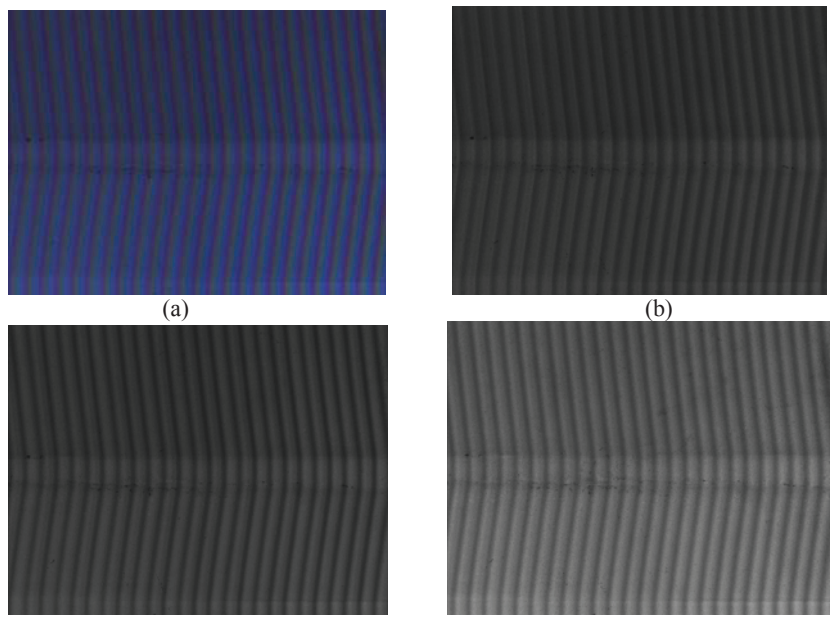

Fig. 2. Captured distorted fringe pattern. (a) Color-encoded distorted fringe pattern; (b) Gray distorted fringe pattern of Red channel; (c) Gray distorted fringe pattern of Green channel; (d) Gray distorted fringe pattern of Blue channel

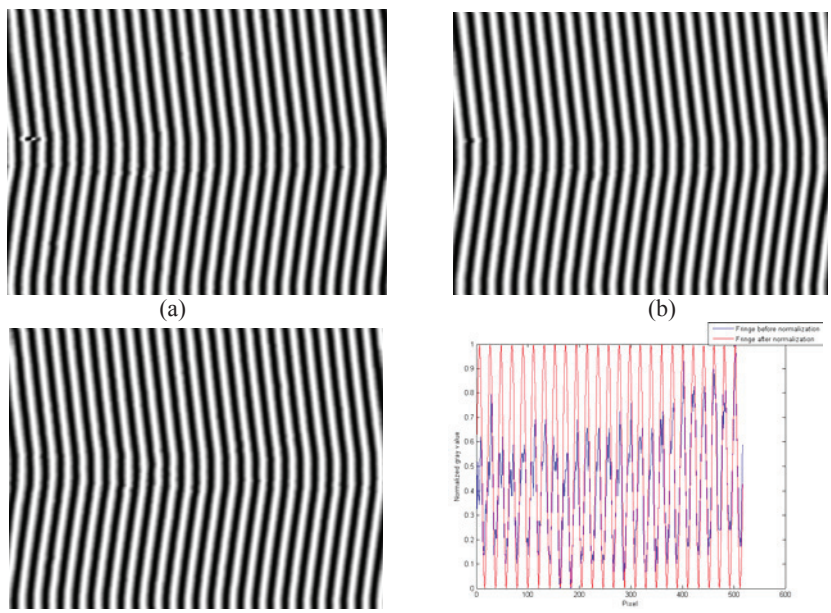

Fig. 3. INFPN operation results. (a) Normalized fringe pattern of Red channel;
(b) Normalized fringe pattern of Green channel; (c) Normalized fringe pattern of Blue channel;
(d) One row of the fringe pattern of Red channel before and after INFPN

After the INFPN operated on each gray fringe pattern, the corrected results are obtained. Normalized fringe pattern of R-G-B channel are shown in Figs. 3(a)-(c), respectively. Figure 3(d) is a 2-D plot of one row of the fringe pattern of Red channel before and after INFPN. The blue curve represents the distorted fringe before INFPN, while the red curve is the distorted fringe after INFPN. It is obviously that the non-sinusoidal distribution, non-uniform brightness and modulation of the captured fringe pattern are effectively corrected. Therefore, the phase errors caused by these factors can be compensated before the fringe pattern is further processed.

A wrapped phase map obtained by the traditional three-step phase-shifting algorithm [Eq. (6)] is shown in Fig. 4(a). Figure 4(b) is the corresponding unwrapped phase map of Fig. 4(a), which is obviously wrong. The wrapped phase map obtained by the RPSA process after INFPN is shown in Fig. 4(c). Figure 4(d) is a 3D plot of the surface profile measurement result (in the form of phase value) of a test object (roof-shaped object) obtained from Fig. 4(c). The accurate and real profile information can be achieved through a sophisticated calibration [13]. The results shown in Fig. 4 certify that the proposed correction strategy which is based on the INFPN and RPSA is able to effectively reduce the phase error in the CFPP even when the original fringe pattern is seriously blurred with gamma distortion, etc. Although some residual errors still exist in the phase map Fig. 4(d), it can be further compensated by some straightforward methods such as LUT.

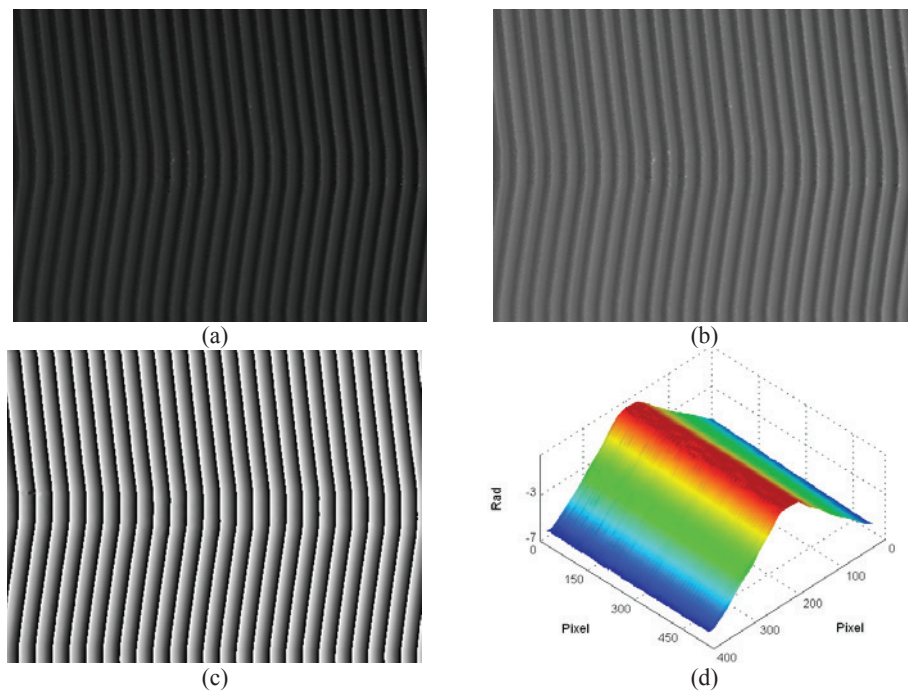

Fig. 4. Measurement results. (a) Wrapped phase map obtained by the traditional three-step phase-shifting algorithm; (b) The corresponding unwrapped phase map of (a); (c) Wrapped phase map obtained by the proposed strategy; (d) 3D plot of the surface profile measurement result (in the form of phase value) of a test object obtained from (c)

4. Conclusions

In this paper, we analyze the causes of the phase error using a LCD or DLP projector in the digital fringe projection profilometry when the CFP technique is utilized to retrieve the phase value. The corresponding phase error corrections are introduced to compensate the deviation of the surface profile measurement as well. The experimental results demonstrate that the phase error can be significantly reduced with our simple correction strategy.

References

[1] M. Takeda and K. Mutoh, “Fourier transform profilometry for the automatic measurement of 3-D object shapes”, *Appl.Opt.*, vol. 22, pp. 3977-3982, 1983.
[2] P. S. Huang and S. Zhang, “Fast three-step phase-shifting algorithm”, *Appl.Opt.*, vol. 45, pp. 5086-5091, 2006.
[3] P. S. Huang, Q. Hu, F. Jin, F. Chiang, “Color-encoded digital fringe projection technique for high-speed three-dimensional surface contouring”, *Opt.Eng.*, vol. 38, pp. 1065-1071, 1999.
[4] S. Zhang, P. S. Huang, “High-resolution real-time three-dimensional shape measurement”, *Opt.Eng.*, vol. 45, pp. 123601-1-8, 2006.
[5] R. W. Wygant, S. P. Almeida and O. D. D. Soares, “Surface inspection via projection interferometry”, *Appl.Opt.*, vol. 27, pp. 4626-4630, 1988.
[6] C. Quan, C. J. Tay, X. Y. He, X. Kang, H. M. Shang, “Microscopic surface contouring by fringe projection method”, *Optics & lasers Technology*, vol. 34, pp. 547-552, 2002.
[7] Z. Zhang, D. P. Towers and C. E. Towers, “Snapshot color fringe projection for absolute three-dimensional metrology of video sequences”, *Appl.Opt.*, vol. 49, pp. 5947-5953, 2010.
[8] S. Zhang and S. Yau, “Generic nonsinusoidal phase error correction for three-dimensional shape measurement using a digital video projector”, *Appl.Opt.*, vol. 46, pp. 36-43, 2007.
[9] H. Cui, X. Chen, N. Dai, T. Yuan, W. Liao, “A new phase error compensation method of 3-D shape measurement system using DMD projector”, *Proc. SPIE, Fourth International Symposium on Precision Mechanical Measurements*, vol. 7130, pp. 713041-1-6, 2008.
[10] Y. Liu, J. Xi, Y. Yu and J. Chicharo, “Phase error correction based on Inverse Function Shift Estimation in Phase Shifting Profilometry using a digital video projector”, *Proc. SPIE, Optical Metrology and Inspection for Industrial Applications,* vol. 7855, pp. 78550W-1-8, 2010.
[11] Y. Hu, J. Xi, J. Chicharo and Z. Yang, “Blind color isolation for color-channel-based fringe pattern profilometry using digital projection”, *J. Opt. Soc. Am. A*, vol. 24, pp. 2372-2382, 2007.
[12] D. C. Ghilia, M. D. Pritt, “Two-Dimensional Phase Unwrapping: Theory, Algorithms, and Software”, *Wiley Press*, 1998.
[13] M. Vo, Z. Wang, T. Hoang and D. Nguyen, “Flexible calibration technique for fringe-projection-based three-dimensional imaging”, *Opt.Let.*, vol. 35, pp. 3192-3194, 2010.
[14] J. A. Quiroga, M. Servin, “Isotropic n-dimensional fringe pattern normalization”, *Opt. Comm.*, vol. 224, pp. 221-227, 2003.
[15] Z. Wang, B. Han, “Advanced iterative algorithm for phase extraction of randomly phase-shifted interferograms”, *Opt. Let.*, vol. 29, pp. 1671-1673, 2004.
[16] Z. Wang, B. Han, “Advanced iterative algorithm for randomly phase-shifted interferograms with intra and inter-frame intensity variations”, *Optics and lasers in Engineering*, vol. 45, pp. 274-280, 2007.